IEEE Access
Multidisciplinary | Rapid Review | Open Access Journal

Received July 17, 2018, accepted August 28, 2018, date of publication September 10, 2018, date of current version October 8, 2018.

Digital Object Identifier 10.1109/ACCESS.2018.2869718

Modeling and Design Empirical Formulas of Microstrip Ridge Gap Waveguide

ABDELMONIEM T. HASSAN[1], MOHAMED A. MOHARRAM HASSAN[1,2], (Member, IEEE), AND AHMED A. KISHK[1], (Fellow, IEEE)

[1]Electrical and Computer Engineering Department, Concordia University, Montreal, QC H4B 1R6, Canada
[2]Electronics and Electrical Communications Engineering Department, Cairo University, Giza 12613, Egypt

Corresponding author: Abdelmoniem T. Hassan (ab_ass@encs.concordia.ca)

ABSTRACT Recently, interest in the microstrip ridge gap waveguide (MRGW) has increased due to the need for a self-packaged and low-loss structures for millimeter-wave applications. The MRGW consists of a grounded textured surface, which is artificially representing a perfect magnetic conductor surface loaded with a thin low dielectric constant substrate with a printed strip. This is topped with another dielectric substrate covered with a conducting plate at the top as a ground plane. Currently, the full-wave and optimization tools are used to design the MRGW structure. Consequently, an efficient modeling and design tool for the MRGW is proposed in this paper via curve fitting. Closed form empirical expressions for the effective dielectric constant, characteristic impedance, and the dispersion effect are provided. The developed expressions are generalized for arbitrarily chosen MRGW parameters. The expressions are verified with the full-wave solution. The results show the potential of the proposed approach in modeling the MRGW structure

INDEX TERMS Gap waveguide, RGW, microstrip, printed RGW, curve fitting.

I. INTRODUCTION

The millimeter-wave frequency band is a potential candidate for various 5G applications [1]. This requires high gain antennas in an array arrangement with an efficient feeding network. Typically, conventional waveguides are used to create a slot antenna array with low loss and high gain [2]. However, at millimeter-wave (mm-wave) frequencies, feeding network design becomes more complicated and difficult to manufacture, especially to maintain the electrical contact between the different metal parts [3], [4]. On the other hand, planar microstrip technologies are also used for implementing antenna array feeding network due to its low cost, compactness, and ease of manufacturing [5]. However, dielectric and radiation losses [6], as well as the possibility of coupling to surface waves, limit the use of such technology [7] at mm-wave frequencies. Surface waves and the spurious radiation of the feeding network affect the radiation characteristic of antenna arrays, such as the sidelobe level and antenna gain. Moreover, the substrate integrated waveguide (SIW) is another guiding structure that was introduced in [8] and has been used at mm-wave frequencies. Basically, SIW resembles the waveguide technology in a printable format. Electromagnetic waves in SIW propagate through the dielectric material with metal on the top and bottom sides and two rows of metallized via holes on the left and right sides [9]. SIW provides the same advantages as the conventional metallic waveguide. However, this guiding structure suffers from dielectric losses, which can be of concern at mm-wave frequancy range.

All the aforementioned limitations can be overcome, especially in the mm-wave range, by using gap waveguide technology introduced in [10]–[12]. The ridge gap waveguide (RGW) concept is based on an air gap sandwiched between two parallel plates, where most of the fields are confined. The bottom plate has a smooth continuous metal (ridge) surrounded by textured surfaces acting as an Artificial Magnetic Conductor (AMC). A smooth metal plate covers the bottom plate with an air gap, acting as the signal ground plane. The gap between these two parallel plates should be smaller than a quarter wavelength at the highest frequency over an operation band to stop the waves over the textured surface and only allow it to propagate between the parallel plates. The main advantages of this technology are the alleviation of dielectric and radiation losses, surface wave suppression and resolving the electrical contact issue between the metal plates at high frequencies. The AMC implementation has been realized using different approaches. It can be implemented using a metal pin (bed of nails) [13] or using mushroom patches

on microstrip substrate [14], which is referred to as printed RGW (PRGW) [15].

Creating arbitrary circuits that have bends and discontinuities is challenging in the RGW and PRGW configurations as this disturbs the bed of nails and mushroom periodicity. This requires adjusting the nails or the mushroom positions. To avoid such a problem, elevating the ridge away from the bed of nails or mushroom surface was proposed without the need to connect the ridge surface to the ground using a thin low dielectric constant substrate. As such, the periodicity of the bed of nails or mushroom is not disturbed, and the signal is propagating in the air-filled guiding structure. Also, the air gap can be filled with a dielectric. In this case, a printed circuit with all the needed discontinuities can be used with its ground and then flipped to face the periodic texture. Such a structure is referred to as inverted microstrip line as the signal is propagating in the dielectric substrate of the microstrip line. The inverted microstrip structure is considered as packaged microstrip line [16], which was treated in several publications [17]–[21]. These are very complicated structures to be analyzed and designed due to the interaction between the periodic structure and the microstrip line. However, they have received more attention because of merging the advantages of the metallic waveguides in term of low losses with the advantages of microstrip technologies in terms of compact size and ease of fabrication. Hence, it can be a preferred candidate for feeding network design at the mm-wave frequency range.

Here, we will consider this structure in its general form where we consider the possibility of filling above and below of the stripline with arbitrary dielectric materials, which will be referred to as MRGW. One of the main obstacles to design the MRGW is the absence of closed-form expressions to calculate or synthesize the characteristic impedance and the effective dielectric constant. Therefore, the design of these lines and components such as power dividers, delay lines, and hybrids is based on numerical tools. In [22] a study with two 90° bends was conducted beside a quadruplet bandpass filter design implemented using MRGW technology without using closed form expressions. Other work using MRGW for antenna array design was implemented to provide high gain using optimization tools [23]. Using optimization tools is time-consuming, especially for antenna array design. The design time can be reduced if closed-form expressions are available. Other work was presented in [24] to investigate the characteristic impedance and modal dispersion equation for metallic ridge gap waveguide in a bed of nails. Moreover, a model for PRGW was presented in [25]; however, the expressions used in that article were based on the ideal PMC and PEC, not for an actual structure, at one frequency.

In this work, we present empirical expressions to model the electrical parameters of the MRGW structure as a function of the physical parameters. The characteristic impedance and propagation constant are modeled with closed-form expressions to facilitate the analysis and synthesis of the present stucuture. Similar to microstrip-line empirical expressions [26], [27], empirical expressions for the MRGW are obtained. The analysis procedure of the MRGW is verified using structures in different scenarios. The main contributions of this work can be summarized as follows:

1) proposing analysis and synthesis formulas for the MRGW to facilitate the design process in Sec. II;
2) introducing general expressions for the effective dielectric constant and characteristic impedance for several possible configurations of the MRGW in Sec II-A;
3) demonstrating the validity of the proposed formulas for various cases of the MRGW in Sec. III; and
4) considering the material dispersion at high frequency into the design formulas in Sec. IV.

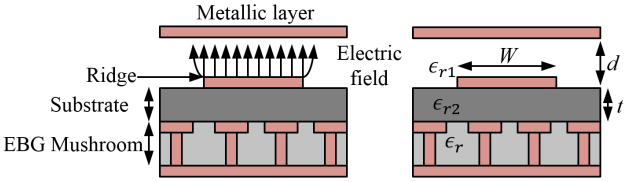

FIGURE 1. Microstrip Ridge Gap Waveguide (MRGW) structure with Electromagnetic Band Gap (EBG) mushroom with arrows indicate the field lines of the quasi-TEM mode.

II. MRGW STRUCTURE AND MODELING

MRGW can be considered as a parallel plate waveguide filled with air or dielectric with thickness d and permittivity ϵ_{r1}, or a microstrip line with possible air substrate. The inner conductor surface of the microstrip line is the surface of the ridge. The microstrip line (ridge) is elevated above the AMC surface by a dielectric spacer that has permittivity ϵ_{r2} and thickness t. The geometry of the MRGW is presented in Fig. 1, which can be seen as an inverted microstrip line enclosed with an AMC. The electric field is mostly within the air gap. However, some of the fringing field lines will be in the substrate. As a consequence, the propagating mode is not a pure transverse electromagnetic mode (TEM), but quasi-TEM. In addition, the substrate material underneath the ridge is nonmagnetic with unity relative magnetic permeability (i.e., $\mu = 1$). An attractive advantage of MRGW configurations with an air gap is that the effective dielectric constant is much smaller than the spacer dielectric constant. Therefore, the loss tangent is substantially reduced, and the component dimensions can be increased, which gives more flexibility in the design at mm-wave frequencies.

A. IMPEDANCE DESIGN FORMULAS

The characteristic impedance equation of the quasi-TEM mode [26], propagating along the MRGW can be express as:

$$Z_c = \frac{120\pi d}{\sqrt{\epsilon_{eff}} W_{eff}} \tag{1}$$

where W_{eff} is the effective width of the line and ϵ_{eff} the effective dielectric constant of the guiding medium. Inspired by the microstrip line analysis expressions, It should be stated that the above expression assumes that the physical parameters are known to get W_{eff} and ϵ_{eff}. Both W_{eff} and ϵ_{eff} are

represented in empirical expressions that contain rational functions of the physical parameters. Using a non-linear curve fitting routine to a microstrip-like, W_{eff} can be expressed as such:

$$\frac{W_{eff}}{d} = \frac{W}{d}\left(\frac{d}{t}+1\right)0.438 + 1.1\ln\left[3.708+\frac{W}{d}\left(\frac{d}{t}+1\right)\right] \quad (2)$$

The effective dielectric constant ϵ_{eff} can be computed by treating the MRGW geometrical configuration as a parallel plate capacitor, which is filled with air and partially filled with a dielectric. This method of analyzing the effective dielectric constant is similar to the method that has been used by Wheeler for the standard microstrip [28]. However, here we considered the effect of the closed structure with AMC. In order to find an accurate empirical expression to estimate ϵ_{eff} we define a function F(d, W) and G(d, W, t) to compensate for the capacitance effect between the top metal, ridge and mushroom such that:

$$\epsilon_{eff} = \frac{\epsilon_{r1}+\epsilon_{r2}}{2}\mathrm{F}(d,W) + \frac{\epsilon_{r1}-\epsilon_{r2}}{2}\mathrm{G}(d,W,t) \quad (3)$$

Using a non-linear curve fitting routine to a microstrip-like ϵ_{eff} can be expressed as:

- If ϵ_{r1}=1

$$\epsilon_{eff} = \frac{\sqrt{\epsilon_{r2}}+\epsilon_{r1}}{2}\left[1+0.0001\left(\frac{W}{d}\right)^{1.041}\right] - \frac{\sqrt{\epsilon_{r2}}-\epsilon_{r1}}{2}\left[\left(1-0.322\left(\frac{d}{W}\right)+2.598\frac{t}{W}\right)^{-1.91} - 1.025\left(1+0.876\left(\frac{W}{t}\right)\right)^{-1.197}\right] \quad (4)$$

- If $1 < \epsilon_{r1} \leq \epsilon_{r2}$

$$\epsilon_{eff} = \frac{\epsilon_{r1}+\epsilon_{r2}}{2}\left[1+0.001\left(\frac{W}{d}\right)^{1.369}\right] - \frac{\epsilon_{r2}-\epsilon_{r1}}{2}\left[\left(1-0.904\left(\frac{d}{W}\right)+2.096\frac{t}{W}\right)^{-0.069} - 0.534\left(1+0.206\left(\frac{W}{t}\right)\right)^{-1.672}\right] \quad (5)$$

- If $\epsilon_{r1} > \epsilon_{r2}$

$$\epsilon_{eff} = \frac{\epsilon_{r1}+\epsilon_{r2}}{2}\left[1-0.0004\left(\frac{W}{d}\right)^{0.987}\right] - \frac{\epsilon_{r2}-\epsilon_{r1}}{2}\left[\left(1-1.428\left(\frac{d}{W}\right)+1.572\frac{t}{W}\right)^{-0.141} - 0.714\left(1+0.126\left(\frac{W}{t}\right)\right)^{-1.986}\right] \quad (6)$$

B. WIDTH DESIGN FORMULAS

An expression for width design can be obtained empirically in terms of rational functions of the physical parameters and the dielectric constant of the material via non-linear curve fitting. Consequently, the MRGW width can be obtained for a given Z_c viz

- If ϵ_{r1}=1

$$\left(\frac{W}{d}\right) = \frac{3.414}{\pi}\left(A+0.062-\ln\left(3.181A+1.663\right) - 0.266\left[\ln(A-1.369)\right]\right) \quad (7)$$

- If $1 < \epsilon_{r1} \leq \epsilon_{r2}$

$$\left(\frac{W}{d}\right) = \frac{3.361}{\pi}\left(A-0.392-\ln\left(0.361A+3.681\right) - 0.354\left[\ln(A-1.283)\right]\right) \quad (8)$$

- If $\epsilon_{r1} > \epsilon_{r2}$

$$\left(\frac{W}{d}\right) = \frac{3.02}{\pi}\left(A-1.544-\ln\left(3.447A-1.933\right) + 1.35\left[\ln(A+1.484)\right]\right) \quad (9)$$

$$A = \frac{120\pi}{\sqrt{\epsilon_{r1}}Z_c} \quad (10)$$

The analysis and synthesis equations were found to be accurate with a maximum error of 6% from the exact theoretical data over the range $\epsilon_{r1}\leq$6.15, $\epsilon_{r2}\leq$10.2, $0.2\leq\frac{t}{d}\leq1$ and $0.1\leq\frac{W}{d}\leq$22.

The MRGW ridge thickness t_h can affect the characteristic impedance and the effective dielectric constant since both are being functions of the MRGW width. According to [29], thick microstrip ($0.05\leq\frac{t_h}{h_m}\leq0.2$) is used for the transmission lines that can be used for quasi-DC operations, however thin line ($0.01\leq\frac{t_h}{h_m}\leq0.05$) is used for the microwave devices, where h_m is the thickness of the substrate in the conventional microstrip line. Similarly, MRGW can be used to design the transmission line for quasi-DC and microwave devices. Therefore, the closed form expressions for the width W_h, considering the effect of the thickness t_h, can be obtained empirically as such:

$$\frac{W_h}{d} = \frac{W}{d} + \frac{0.8t_h}{d\pi}\left[1+\ln\left(\frac{2d}{t_h}\right)\right] \quad (11)$$

In [30] It has been noticed that Z_c value decreases as the strip thickness increases. Therefore, the effect of the finite thickness of the MRGW line may be thought of as an increase in width. Equation (11) is similar to the one used for the conventional microstrip in [31]. However, different coefficients are used in (11) since the estimation of $\frac{W}{d}$ in MRWG is different from the conventional microstrip line. When the line thickness is considered, the W term in (2),(4),(5) and (6) needs to be replaced by W_h, which can be obtained from (11).

C. PORT DEFINITION AND DATA EXTRACTION

The definition of the waveguide port used for MRWG is similar to the definition in [32], with port width dimensions of at least one unit cell period p from both sides of the MRGW line

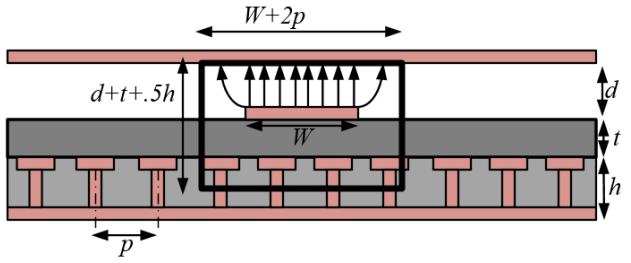

FIGURE 2. Port definition for the MRGW.

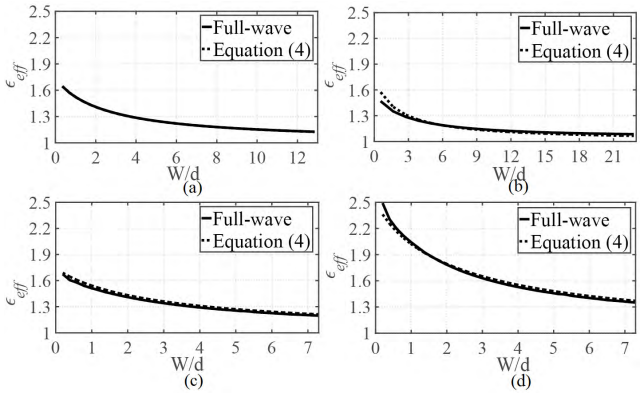

FIGURE 3. The effective dielectric constant when ϵ_{r1} is an air: (a) case A, (b) case B, (c) case C and (d) case D.

in the transverse direction. Hence, most of the fields (confined and fringing) are considered. Also, the port length is designed to cover the gap region d ,substrate t and half of the mushroom pin height h in the longitudinal direction as shown in Fig. 2. The propagation constant β and Z_c can be obtained directly from the waveguide port information using full-wave analysis at a certain frequency. The relation between β and ϵ_{eff} can be found in [33] for quasi-TEM. Then the empirical expressions are developed by using curve fitting.

III. EQUATIONS VERIFICATION

To verify the proposed formulas, different cases have been studied based on ϵ_{r1} and ϵ_{r2}. First, the case when ϵ_{r1} is air, the MRGW structure in [22] is used. The unit cells are designed to provide a stopband between 20-40 GHz loaded with $\epsilon_r = 3$. The unit cell with $\epsilon_{r2} = 3$ is used in case A. On the other hand, a unit cell for stopband 50-80 GHz with $\epsilon_{r2} = 3$ is also used with the thickness = 0.13 mm and the air gap = 0.18 mm. The mushroom is designed with radius = 0.7 mm, via diameter = 0.33 mm, period = 0.85 mm and loaded with $\epsilon_r = 3$ in case B. Moreover, a unit cell for stopband 10-20 GHz with $\epsilon_{r2} = 3$ is also used with the thickness = 0.508 mm and the air gap = 0.508 mm. The mushroom is designed with radius = 1.3 mm, via diameter = 0.3 mm, period = 3 mm and loaded with $\epsilon_r = 3$ in case C. The same dimensions that used in case C are used for case D, however, with $\epsilon_{r2} = 6.15$ is used.

Then, ϵ_{eff} is calculated using (4) and compared with the full-wave analysis of the different cases (A,B,C,D) at the center frequencies 30 GHz, 60 GHz and 14 GHz, respectively. The variation of the ϵ_{eff} with $\frac{W}{d}$ is shown in Fig. 3.

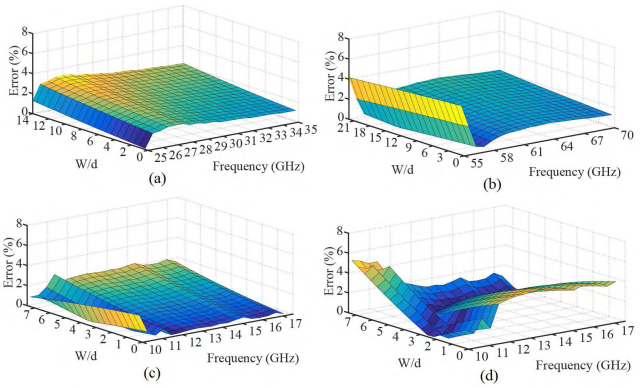

FIGURE 4. The error when ϵ_{r1} is an air: (a) case A, (b) case B, (c) case C and (d) case D.

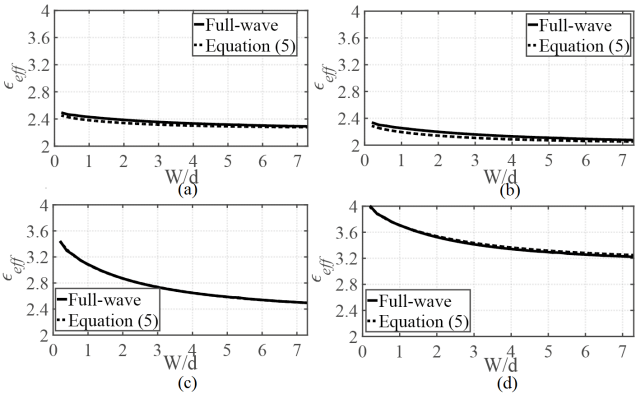

FIGURE 5. The effective dielectric constant when the gap is filled with dielectric ($\epsilon_{r1} < \epsilon_{r2}$): (a) case E, (b) case F, (c) case G and (d) case H.

It may be observed that the empirical expressions are in a good agreement with the full-wave analysis results within a maximum error of less than 5% as shown in Fig. 4. Also, it may be noticed that, the value of ϵ_{eff} gets close to one when the width of the MRGW line increases because most of the electric field becomes more confined within the air gap. From the different cases it can be observed that the approximation of using $\epsilon_{eff} = 1$ is no longer valid, especially when the value of ϵ_{r2} is high.

Since the empirical formulas are generalized to accommodate the gap filled with dielectric martial, several MRGW unit cells are used for verification. When $\epsilon_{r1} < \epsilon_{r2}$, a unit cell is designed to provide stop band between 8-18 GHz. A substrate dielectric material is used with $\epsilon_{r2} = 3$ and thickness = 0.508 mm. The gap thickness = 0.508 mm is filled with substrate dielectric martial that has $\epsilon_{r1} = 2.2$ and $\epsilon_{r1} = 1.96$ for case E and case F, respectively. The EBG mushroom has the same dimensions as case C to provide the required stop band. Moreover, another unit cell for the case when $\epsilon_{r1} < \epsilon_{r2}$ are designed to provide stopband between 8-18 GHz with $\epsilon_{r2} = 6.15$ and thickness = 0.508 mm. The gap thickness of 0.508 mm is filled with substrate dielectric martial that has permittivity $\epsilon_{r1} = 2.2$ and $\epsilon_{r1} = 3$ for case G and case H, respectively. The variation of ϵ_{eff} over the line width at 14 GHz is shown in Fig. 5. From the results, it may be observed that the value of ϵ_{eff} gets close to the substrate

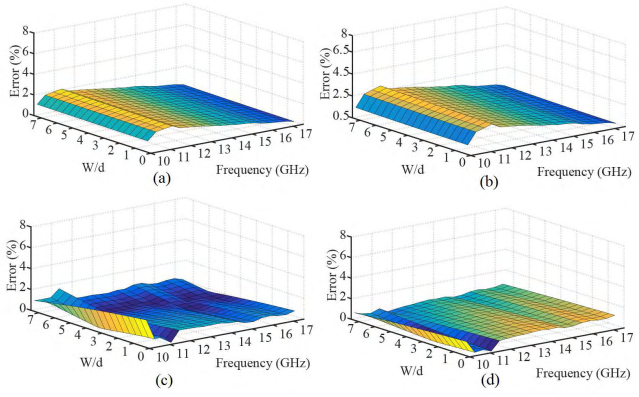

FIGURE 6. The error when the gap is filled with dielectric ($\epsilon_{r1} < \epsilon_{r2}$): (a) case E, (b) case F, (c) case G and (d) case H.

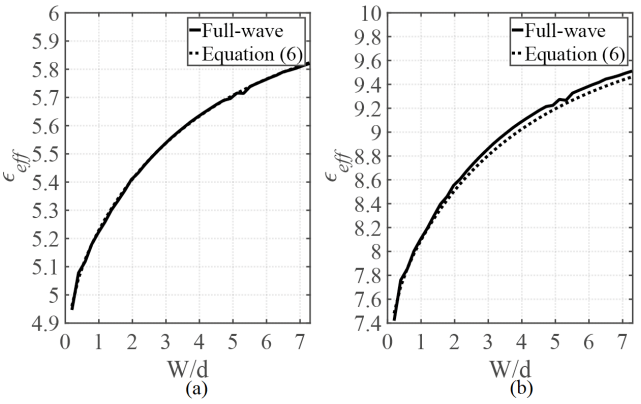

FIGURE 7. The effective dielectric constant when the an air gap is filled with dielectric ($\epsilon_{r1} > \epsilon_{r2}$): (a) case X and (b) case Y.

dielectric permittivity filling the gap as the width of MRGW line increases. As expected, most of the electric field becomes more confined within the layer between the top metal and the ridge. The values obtained from the empirical expressions are in good agreement with the full-wave analysis results in a maximum error of 3% as shown in Fig. 6. The error has been calculated as an absolute percentage error with respect to the values obtained from the full-wave analysis.

On the other hand, the case when $\epsilon_{r1} > \epsilon_{r2}$ is verified through different MRGW unit cells. A unit cell is designed to provide stop band between 8-18 GHz with $\epsilon_{r1} = 6.15$ and $\epsilon_{r2} = 3$ each with thickness $= 0.508$ mm in case X. Another unit cell is designed to provide stop band between 8-18 GHz with $\epsilon_{r1} = 10.2$, and $\epsilon_{r2} = 3$ and both substrates have thickness $= 0.508$ mm in case Y. The EBG mushroom is designed with the same dimensions as case C. Then, the variation of ϵ_{eff} over the line width at 14 GHz is shown in Fig. 7. From the results, it may be observed that the value of ϵ_{eff} increases as the line width increases, which is similar to the behavior of the microstrip. The values obtained from the empirical expressions are in good agreement with the full-wave analysis results within a maximum error of 2% as shown in Fig. 8.

The design expressions for the width are also verified by known Z_c. Using the previous unit cell structures, the estimation of MRGW width is calculated using (7),(8) and (9).

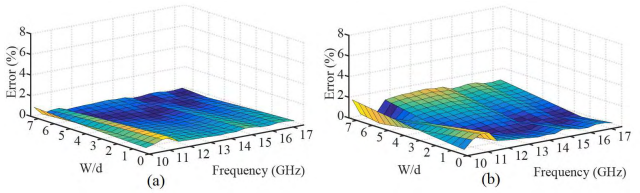

FIGURE 8. The error when the an air gap is filled with dielectric ($\epsilon_{r1} > \epsilon_{r2}$): (a) case X and (b) case Y.

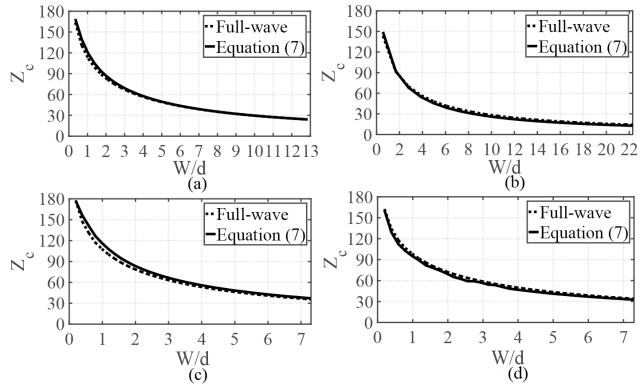

FIGURE 9. The characteristic impedance Z_c of the MRGW with an air gap: (a) case A, (b) case B, (c) case C and (d) case D.

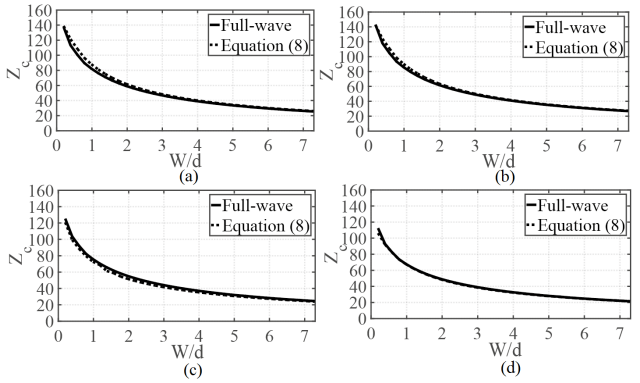

FIGURE 10. The characteristic impedance Z_c of the MRGW with an air gap filled with substrate dielectric ($\epsilon_{r1} < \epsilon_{r2}$): (a) case E, (b) case F, (c) case G and (d) case H.

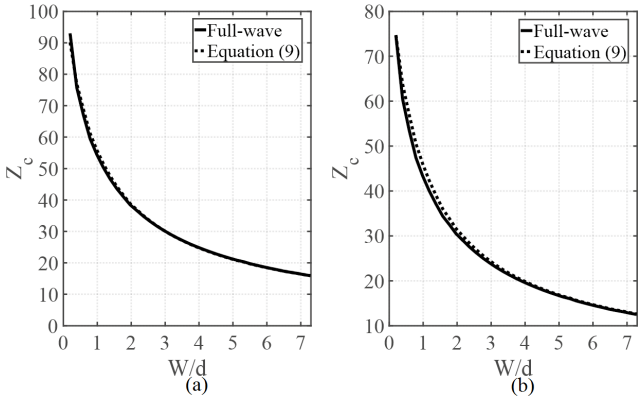

FIGURE 11. The characteristic impedance Z_c of the MRGW with an air gap filled with substrate dielectric ($\epsilon_{r1} > \epsilon_{r2}$): (a) case X and (b) case Y.

Fig. 9–11 show the characteristic impedance calculated from the full-wave analysis and the empirical expressions. Good agreement between the empirical expression and the

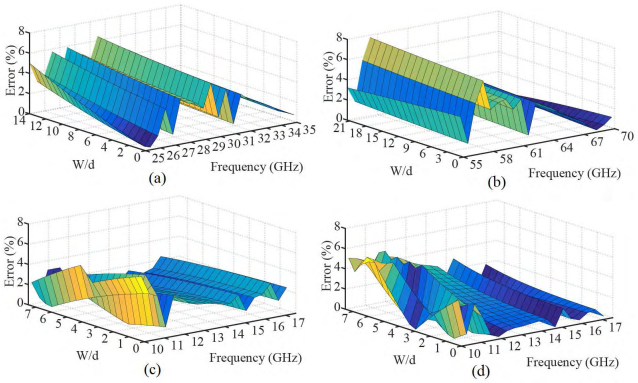

FIGURE 12. The error for Z_c of the MRGW with an air gap: (a) case A, (b) case B, (c) case C and (d) case D.

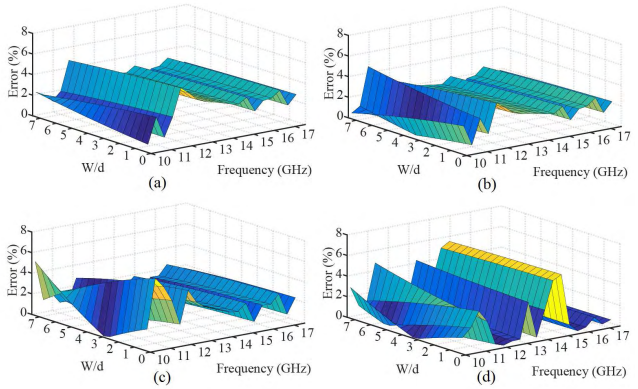

FIGURE 13. The error for Z_c of the MRGW with an air gap filled with substrate dielectric ($\epsilon_{r1} < \epsilon_{r2}$): (a) case E, (b) case F, (c) case G and (d) case H.

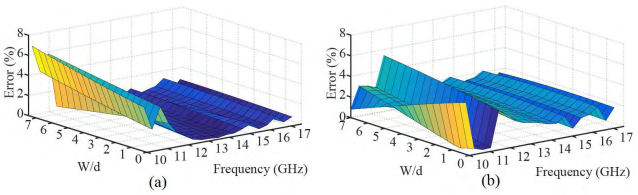

FIGURE 14. The error for Z_c of the MRGW with an air gap filled with substrate dielectric ($\epsilon_{r1} > \epsilon_{r2}$): (a) case X and (b) case Y.

full-wave results can be observed within a maximum error of less than 8% as shown in Fig. 12–14. Also as expected, the larger MRGW width is, the lower the characteristic impedance is. Besides, in the case of filling the gap with dielectric martial, it can be observed that the dimensions (width of the line) are getting smaller for specific Z_c compared with the case of air filled. Also, it can be observed that the thickness of the dielectric underneath the ridge with ϵ_{r2} has negligible effect on calculating Z_c, since most of the fields are concentrated at the gap between the top metal plate and the ridge. For example, in case C and case D the thickness of the substrate dielectric underneath the ridge is 0.508 mm with different ϵ_{r2} but the width for $Z_c = 50\Omega$ is approximately 2 mm for both. It is important to mention that case C, case G and case Y were used for data fitting, however, the other cases used for testing. Since the empirical equations are frequency independent, it may be pointed out

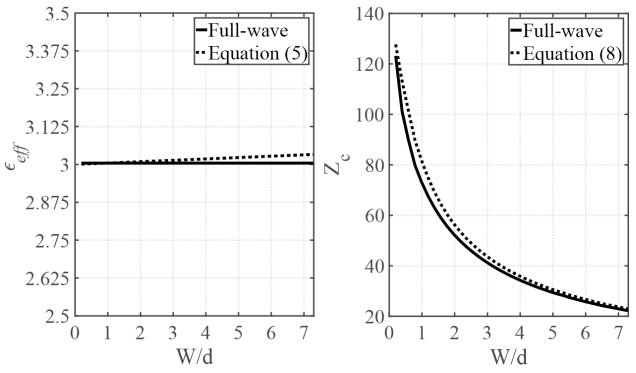

FIGURE 15. The effective dielectric constant and the characteristic impedance of the MRGW when the gap is filled with dielectric ($\epsilon_{r1} = \epsilon_{r2}$), (case Z).

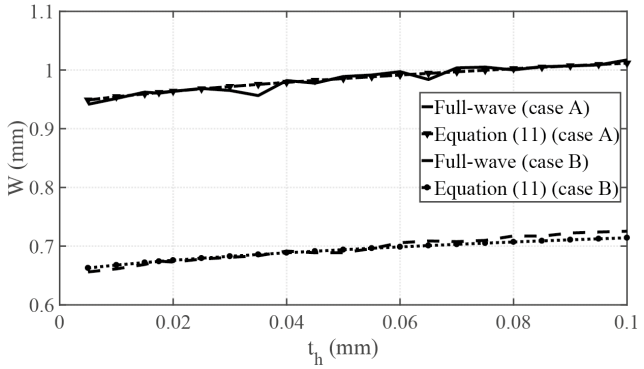

FIGURE 16. The effect of the thickness on the width of the MRGW.

that the variation of Z_c and ϵ_{eff} with the frequency (within the stop band) is small for certain width that shows less dispersion as it will be discussed in the next section.

Finally, for the case where $\epsilon_{r1} = \epsilon_{r2}$, The same dimensions in case C are used in the unit cell. However, both the gap and the dielectric martial underneath the ridge have $\epsilon_{r1} = \epsilon_{r2} = 3$ in case Z. As expected the confined field within the gap and the fringing will experience the same material such that the ϵ_{eff} will be almost 3 as shown in Fig. 15.

The effect of MRGW line thickness is verified in Fig. 16 where the empirical expression (11) is used and compared with the full-wave analysis. It can be noticed that the change of the width versus MRGW thickness is very small. The width of MRGW in case A is selected to give 58Ω with zero thickness. However, the thickness variation changes the impedance up to -5Ω. On the other hand, the width of the MRGW in case B is selected to give 54Ω with zero thickness, by including the effect of the thickness, up to -3Ω of variation can be observed.

Moreover, a comparison between the present work and previously published work using MRGW is conducted, in a way that we compare the values obtained from our model with these used the other works. In [23] the line width for $Z_c = 50\Omega$, quarter wavelength transformer length and width were 0.9 mm, 2.5 mm and 1.6 mm respectively. However, the values obtained from our model are 1.06 mm, 2.22 mm and 1.8 mm respectively. It can be

pointed out that the difference between our model values and those in [23] is due to the correction used in [23] to account for discontinuities using optimization. It is worth to mention that our model values were close to the optimized values which mean the optimizer will start from good guest and reduce the processing time. Also in [32] where $\frac{t}{d} = 2$ the line width for $Z_c = 50\Omega$ was 0.78 mm where the value of our model is 0.71 mm. The AMC layer can be implemented using metal pins instead of EBG mushroom, in [34] the line width for $Z_c = 50\Omega$ was 1.11 mm and the value of our model is 1.06 mm, also in [35] where MRGW technology is used with metal pins to design 4x4 planar dual-mode horn array, the line width for $Z_c = 50\Omega$ was 7.362 mm and from our model is 6.812 mm, whereas, for the power divider line width for $Z_c = 50\Omega$ changed to 8.8 mm. The quarter wavelength transformer length and width for $Z_c = 70\Omega$ were 6.6 mm and 4.39 mm, respectively. However, the values obtained from our model are 6.1 mm and 3.5 mm respectively at 10.5 GHz. Another line for $Z_c = 100\Omega$ is used with width 2.4 mm and the value of our model is 1.6 mm where the effect of the continuity is not included.

IV. DISPERSION AT HIGH FREQUENCY

The empirical formulas for the characteristic impedance and the effective dielectric constant are obtained based on the quasi-TEM mode of propagation. Within a limited frequency band, the quasi-TEM mode changes linearly with the frequency. However, beyond a specific frequency (cutoff), other modes propagate (TM, TE and hybrid coupling of TM and TE modes). Each mode has different propagation parameter from the other in terms of velocity and wave impedance. Accordingly, the characteristic impedance and the effective dielectric constant will change over the frequency and show dispersive characteristics. Fortunately, MRGW is designed to work within a specific frequency band where the quasi-TEM is the only propagating mode. Therefore, the signal suffers from less dispersion than other TE or TM-based guiding structures.

Wideband Debye and multi-pole Debye models are used to characterize the dielectric constant [36]. Also, stop band frequencies from zero up to the cutoff frequency are achieved by using PMC instead of AMC. The structure parameters such as the air gap and substrate thickness are playing a crucial role to determine the cutoff frequency. Then the variations of the characteristic impedance and the effective dielectric constant over the frequency are shown in Fig. 17 and Fig. 18 respectively.

From Fig. 17, in case A $\epsilon_{r2} = 3$ is used with air gap such that a stop band of 0-40 GHz is obtained. The width of the ridge is selected to give 54Ω. However, in case B $\epsilon_{r2} = 3$ is used for the substrate and the air gap space is selected to give stop band over 0-80 GHz. The width of the ridge is selected to give 60Ω. In Fig. 18, high permittivity $\epsilon_{r1} = 6.15$ and $\epsilon_{r2} = 3$ are used. It may be observed that the variations of the characteristic impedance and the effective dielectric constant over the frequency are very small. The MRGW

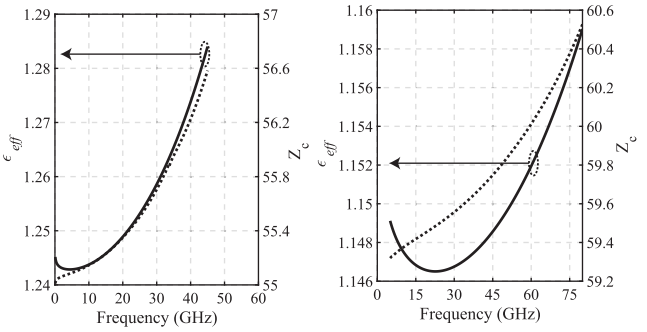

FIGURE 17. The dispersion of the MRGW with an air gap(the left for (case A) and the right for (case B)).

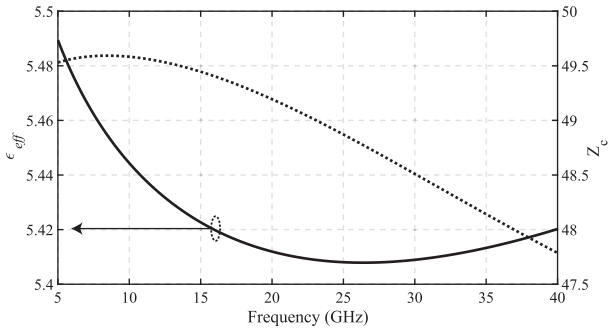

FIGURE 18. The dispersion of the MRGW with an air gap filled with substrate dielectric permittivity.

width is selected to have a characteristic impedance of 50Ω. The thickness of the substrates is selected to give a stop band over 0-25 GHz along with the PMC. Within the whole stop band, the variations of the characteristic impedance and the effective dielectric constant are very small and become more observable after the cutoff frequency as expected because the fields are not bounded by AMC walls, and other modes of propagation are excited.

V. CONCLUSION

We have presented empirical expressions to analyze and design the MRGW for the propagating quasi-TEM mode. The MRGW supports quasi-TEM as a propagating mode imposed by the AMC. The obtained expressions have been inspired by the microstrip line well-known design expressions. These empirical expressions are generalized to be used in case of the gap filled with dielectric material. The estimation of the characteristic impedance and the effective dielectric constant have shown good agreement with the full-wave analysis. Unlike Microstrip line, it has been observed that the MRGW has less dispersive behavior within the stop band.

REFERENCES

[1] Z. Pi, J. Choi, and R. W. Heath, Jr., "Millimeter-wave gigabit broadband evolution toward 5G: Fixed access and backhaul," *IEEE Commun. Mag.*, vol. 54, no. 4, pp. 138–144, Apr. 2016.

[2] Y. Miura, J. Hirokawa, M. Ando, Y. Shibuya, and G. Yoshida, "Double-layer full-corporate-feed hollow-waveguide slot array antenna in the 60-GHz band," *IEEE Trans. Antennas Propag.*, vol. 59, no. 8, pp. 2844–2851, Aug. 2011.

[3] P.-S. Kildal, A. U. Zaman, E. Rajo-Iglesias, E. Alfonso, and A. V. Nogueira, "Design and experimental verification of ridge gap waveguide in bed of nails for parallel-plate mode suppression," *IET Microw., Antennas Propag.*, vol. 5, no. 3, pp. 262–270, Mar. 2011.

[4] E. Rajo-Iglesias and P.-S. Kildal, "Numerical studies of bandwidth of parallel-plate cut-off realised by a bed of nails, corrugations and mushroom-type electromagnetic bandgap for use in gap waveguides," *IET Microw., Antennas Propag.*, vol. 5, no. 3, pp. 282–289, Mar. 2011.
[5] I. J. Bahl and D. K. Trivedi, "A designer's guide to microstrip line," *Microwaves*, vol. 16, pp. 174–182, May 1977.
[6] F. E. Gardiol, "Radiation from microstrip circuits: An introduction," *Int. J. Microw. Millim.-Wave Comput.-Aided Eng.*, vol. 1, no. 2, pp. 225–235, 1991.
[7] P.-S. Kildal, "Three metamaterial-based gap waveguides between parallel metal plates for mm/submm waves," in *Proc. 3rd Eur. Conf. Antennas Propag.*, Berlin, Germany, Mar. 2009, pp. 28–32.
[8] J. Hirokawa and M. Ando, "Single-layer feed waveguide consisting of posts for plane TEM wave excitation in parallel plates," *IEEE Trans. Antennas Propag.*, vol. 46, no. 5, pp. 625–630, May 1998.
[9] D. Deslandes and K. Wu, "Accurate modeling, wave mechanisms, and design considerations of a substrate integrated waveguide," *IEEE Trans. Microw. Theory Techn.*, vol. 54, no. 6, pp. 2516–2526, Jun. 2006.
[10] E. Pucci, E. Rajo-Iglesias, and P.-S. Kildal, "New microstrip gap waveguide on mushroom-type EBG for packaging of microwave components," *IEEE Microw. Wireless Compon. Lett.*, vol. 22, no. 3, pp. 129–131, Mar. 2012.
[11] H. Raza, J. Yang, P.-S. Kildal, and E. Alfonso, "Resemblance between gap waveguides and hollow waveguides," *IET Microw., Antennas Propag.*, vol. 7, no. 15, pp. 1221–1227, Dec. 2013.
[12] P.-S. Kildal, "Waveguides and transmission lines in gaps between parallel conducting surfaces," EP Patent 2009 057 743, Jun. 22, 2009.
[13] M. G. Silveirinha, C. A. Fernandes, and J. R. Costa, "Electromagnetic characterization of textured surfaces formed by metallic pins," *IEEE Trans. Antennas Propag.*, vol. 56, no. 2, pp. 405–415, Feb. 2008.
[14] D. Sievenpiper, L. Zhang, R. F. J. Broas, N. G. Alexopolous, and E. Yablonovitch, "High-impedance electromagnetic surfaces with a forbidden frequency band," *IEEE Trans. Microw. Theory Techn.*, vol. 47, no. 11, pp. 2059–2074, Nov. 1999.
[15] S. A. Razavi, P.-S. Kildal, L. Xiang, E. A. Alós, and H. Chen, "2×2-slot element for 60-GHz planar array antenna realized on two doubled-sided PCBs using SIW cavity and EBG-type soft surface fed by microstrip-ridge gap waveguide," *IEEE Trans. Antennas Propag.*, vol. 62, no. 9, pp. 4564–4573, Sep. 2014.
[16] E. Rajo-Iglesias, A. U. Zaman, and P.-S. Kildal, "Parallel plate cavity mode suppression in microstrip circuit packages using a lid of nails," *IEEE Microw. Wireless Compon. Lett.*, vol. 20, no. 1, pp. 31–33, Jan. 2010.
[17] A. Kishk, A. U. Zaman, and P.-S. Kildal, "Numerical prepackaging with PMC lid—Efficient and simple design procedure for microstrip circuits including the packaging," *ACES J.*, vol. 27, no. 5, pp. 389–398, May 2012.
[18] J. Zhang, X. Zhang, D. Shen, and A. A. Kishk, "Packaged microstrip line: A new quasi-TEM line for microwave and millimeter-wave applications," *IEEE Trans. Microw. Theory Techn.*, vol. 65, no. 3, pp. 707–719, Mar. 2017.
[19] J. Zhang, X. Zhang, D. Shen, and A. A. Kishk, "A novel self-packaged microstrip line," in *Proc. 32nd URSI Gen. Assem. Sci. Symp.*, Montreal, QC, Canada, Aug. 2017, pp. 1–2.
[20] J. Zhang, X. Zhang, D. Shen, and A. A. Kishk, "Design of packaged microstrip line," in *Proc. IEEE Int. Conf. Microw. Millim. Wave Technol. (ICMMT)*, Beijing, China, Jun. 2016, pp. 82–84.
[21] M. S. Sorkherizi and A. A. Kishk, "Self-packaged, low-loss, planar bandpass filters for millimeter-wave application based on printed gap waveguide technology," *IEEE Trans. Compon., Packag., Manuf. Technol.*, vol. 7, no. 9, pp. 1419–1431, Sep. 2017.
[22] M. S. Sorkherizi and A. A. Kishk, "Fully printed gap waveguide with facilitated design properties," *IEEE Microw. Wireless Compon. Lett.*, vol. 26, no. 9, pp. 657–659, Sep. 2016.
[23] M. S. Sorkherizi, A. Dadgarpour, and A. A. Kishk, "Planar high-efficiency antenna array using new printed ridge gap waveguide technology," *IEEE Trans. Antennas Propag.*, vol. 65, no. 7, pp. 3772–3776, Jul. 2017.
[24] A. Polemi and S. Maci, "Closed form expressions for the modal dispersion equations and for the characteristic impedance of a metamaterial-based gap waveguide," *IET Microw., Antennas Propag.*, vol. 4, no. 8, pp. 1073–1080, Aug. 2010.
[25] M. M. M. Ali, S. I. Shams, and A. R. Sebak, "Printed ridge gap waveguide 3-dB coupler: Analysis and design procedure," *IEEE Access*, vol. 6, pp. 8501–8509, 2018.
[26] E. Hammerstad and O. Jensen, "Accurate models for microstrip computer-aided design," in *IEEE MTT-S Int. Microw. Symp. Dig.*, Washington, DC, USA, May 1980, pp. 407–409.
[27] M. Kirschning and R. H. Jansen, "Accurate wide-range design equations for the frequency-dependent characteristic of parallel coupled microstrip lines," *IEEE Trans. Microw. Theory Techn.*, vol. MTT-32, no. 1, pp. 83–90, Jan. 1984.
[28] H. A. Wheeler, "Transmission-line properties of a strip on a dielectric sheet on a plane," *IEEE Trans. Microw. Theory Techn.*, vol. MTT-25, no. 8, pp. 631–647, Aug. 1977.
[29] M. A. R. Gunston and J. R. Weale, "Variation of microstrip impedance with strip thickness," *Electron. Lett.*, vol. 5, no. 26, pp. 697–698, Dec. 1969.
[30] M. A. R. Gunston and J. R. Weale, "Transmission characteristics of microstrip," *Marconi Rev.*, vol. 32, pp. 226–243, Oct./Dec. 1969.
[31] I. J. Bahl and R. Garg, "Simple and accurate formulas for a microstrip with finite strip thickness," *Proc. IEEE*, vol. 65, no. 11, pp. 1611–1612, Nov. 1977.
[32] N. Bayat-Makou and A. A. Kishk, "Millimeter-wave substrate integrated dual level gap waveguide horn antenna," *IEEE Trans. Antennas Propag.*, vol. 65, no. 12, pp. 6847–6855, Dec. 2017.
[33] R. E. Collin, *Foundations for Microwave Engineering*, 2nd ed. New York, NY, USA: McGraw-Hill, 1992.
[34] A. A. Brazález, E. Rajo-Iglesias, J. L. Vázquez-Roy, A. Vosoogh, and P.-S. Kildal, "Design and validation of microstrip gap waveguides and their transitions to rectangular waveguide, for millimeter-wave applications," *IEEE Trans. Microw. Theory Techn.*, vol. 63, no. 12, pp. 4035–4050, Dec. 2015.
[35] E. Pucci, E. Rajo-Iglesias, J. L. Vázquez-Roy, and P.-S. Kildal, "Planar dual-mode horn array with corporate-feed network in inverted microstrip gap waveguide," *IEEE Trans. Antennas Propag.*, vol. 62, no. 7, pp. 3534–3542, Jul. 2014.
[36] A. R. Djordjevic, R. M. Biljie, V. D. Likar-Smiljanic, and T. K. Sarkar, "Wideband frequency-domain characterization of FR-4 and time-domain causality," *IEEE Trans. Electromagn. Compat.*, vol. 43, no. 4, pp. 662–667, Nov. 2001.

ABDELMONIEM T. HASSAN was born in Khartoum, Sudan. He received the B.Sc. degree in electronics and communications engineering from the University of Khartoum in 2012 and the M.Sc. degree in electrical engineering from the King Fahd University of Petroleum and Minerals, Dhahran, Saudi Arabia, in 2016. He is currently pursuing the Ph.D. degree with Concordia University, Montreal, QC, Canada. His current research interests include ridge gap guiding structures, modeling electromagnetic problems, and MIMO antenna systems.

MOHAMED A. MOHARRAM HASSAN (S'11–M'16) received the B.Sc. (Hons.) and M.Sc. degrees in electronics and communications engineering from Cairo University, Giza, Egypt, in 2008 and 2011, respectively, and the Ph.D. degree from Concordia University, Montreal, QC, Canada, in 2015. From 2008 to 2011, he served as a Teaching and Research Assistant with the Department of Electronics and Communications Engineering, Cairo University. From 2011 to 2015, he was a Research Assistant with Concordia University, where he was a Post-Doctoral Fellow until 2018. He is currently a post-doctoral fellow with the École Polytechnique de Montréal, Montréal, Quebéc, Canada. He is also an Assistant Professor with the Electronics and Communications Engineering Department, Cairo University, Egypt.

He received the FRQNT Post-Doctoral Research Fund in 2018. His research interests include antenna design and measurement, computational electromagnetics, and microwave components design. He received the First Place Award from the Centre de Recherche En Electronique Radiofrequence 2015 Poster Competition, Montreal, Canada. He also received an Honorable Mention in the Student Paper Competition from the 2015 IEEE AP-S Symposium on Antennas and Propagation. He was a recipient of the Young Scientist Award presented at the 2017 URSI General Assembly. He served as a reviewer for the IEEE journals and magazines.

AHMED A. KISHK (S'84–M'86–SM'90–F'98) received the B.S. degree in electronic and communication engineering from Cairo University, Cairo, Egypt, in 1977, the B.Sc. degree in applied mathematics from Ain-Shams University, Cairo, in 1980, and the M.Eng. and Ph.D. degrees from the Department of Electrical Engineering, University of Manitoba, Winnipeg, Canada, in 1983 and 1986, respectively. From 1977 to 1981, he was a Research Assistant and an Instructor with the Faculty of Engineering, Cairo University. From 1981 to 1985, he was a Research Assistant with the Department of Electrical Engineering, University of Manitoba. From 1985 1986, he was a Research Associate Fellow with the Department of Electrical Engineering, University of Manitoba. In 1986, he joined the Department of Electrical Engineering, The University of Mississippi, as an Assistant Professor. He was on sabbatical leave with the Chalmers University of Technology, Sweden, from 1994 to 1995 and from 2009 to 2010 academic years. He was a Professor with The University of Mississippi (1995–2011). He was the Director of the Center for Applied Electromagnetic System Research from 2010 to 2011. He has been a Professor with Concordia University, Montreal, QC, Canada, since 2011, as the Tier 1 Canada Research Chair in advanced antenna systems. He is currently a Distinguish Lecturer with the Antennas and Propagation Society (2013–2015). He has published over 290-refereed journal articles and 450 conference papers. He has a co-authored four books and several book chapters. He offered several short courses in international conferences. His research interests include the areas of design of dielectric resonator antennas, microstrip antennas, small antennas, microwave sensors, RFID antennas for readers and tags, multi-function antennas, microwave circuits, EBG, artificial magnetic conductors, soft and hard surfaces, phased array antennas, computer aided design for antennas, design of millimeter frequency antennas, and feeds for parabolic reflectors. He was a Technical Program Committee Member of several international conferences. He was a member of the AP AdCom (2013–2015). He was the 2017 AP President. He is currently a member of the Antennas and Propagation Society, the Microwave Theory and Techniques Society, the Sigma Xi Society, the U.S. National Committee of International Union of Radio Science Commission B, the Phi Kappa Phi Society, the Electromagnetic Compatibility Society, and the Applied Computational Electromagnetics Society. In recognition for contributions and continuous improvements in teaching and research to prepare students for future careers in antennas and microwave circuits, he has been a fellow of the IEEE since 1998, and fellow of the Electromagnetic Academy and the Applied Computational Electromagnetic Society (ACES). He and his students received several awards. He was a recipient of the 1995 and 2006 Outstanding Paper Awards for papers published in *The Applied Computational Electromagnetic Society* journal. He received the 1997 Outstanding Engineering Educator Award from Memphis Section of the IEEE, the Outstanding Engineering Faculty Member of the Year in 1998 and 2009, the Faculty Research Award for outstanding performance in research in 2001 and 2005, and the Award from the Distinguished Technical Communication for the entry of the *IEEE Antennas and Propagation Magazine* in 2001. He also received The Valued Contribution Award for the outstanding invited presentation–EM Modeling of Surfaces with STOP or GO Characteristics–Artificial Magnetic Conductors and Soft and Hard Surfaces–from the Applied Computational Electromagnetic Society. He received the Microwave Prize 2004 from the Microwave Theory and Techniques Society. He received the 2013 Chen-To Tai Distinguished Educator Award from the IEEE Antennas and Propagation Society. He was the Chair of Physics and Engineering Division, Mississippi Academy of Science (2001–2002). He was an Associate Editor of *Antennas and Propagation* news letters from 1990 to 1993. He was an Editor of the *IEEE Antennas and Propagation Magazine* (1993–2014). He was also an Editor of the ACES journal in 1997. He was an Editor-in-Chief of the ACES Journal from 1998 to 2001. He was the Co-Editor of the special issue on Advances in the Application of the Method of Moments to Electromagnetic Scattering Problems in the ACES journal. He was a Guest Editor of the special issue on artificial magnetic conductors, soft/hard surfaces, and other complex surfaces, in the IEEE TRANSACTIONS ON ANTENNAS AND PROPAGATION, in 2005. He is the editor of three books.